INVESTIGATION OF THE SILICON PHOTOMULTIPLIERS SUITABILITY FOR RADIATION DETECTION

by

ALİ OSMAN ÇETİNKAYA

THESIS SUBMITTED TO

THE GRADUATE SCHOOL OF NATURAL AND APPLIED SCIENCES

OF

THE ABANT IZZET BAYSAL UNIVERSITY

IN PARTIAL FULFILLMENT OF THE REQUIREMENTS FOR THE

DEGREE OF

MASTER OF SCIENCE

IN

THE DEPARTMENT OF PHYSICS

JANUARY 2015

Approval of the Graduate School of Natural Sciences

Prof. Dr. Duran KARAKAŞ

Director

I certify that this thesis satifies all the requirements as a thesis for the degree of Master of Science.

Prof. Dr. İbrahim Belenli

Head of Physics Department

This is to certify that we have read this thesis and that in our opinion it is fully adequate, in scope and quality as a thesis for the degree of Master of Science.

Assist. Prof. Dr. Aliekber Aktağ

Co-Supervisor

Prof. Dr. Ercan Yılmaz

Supervisor

Examining Committee Members

1. Prof. Dr. Ercan YILMAZ .....
2. Assoc. Prof. Dr. Hüseyin KARAÇALI .....
3. Assist. Prof. Dr. Aliekber AKTAĞ .....
4. Assist. Prof. Dr. Nuray ER .....
5. Assist. Prof. Dr. Oktay AYTAR .....

To my sweet family members;

My parents, Mükerrem and Sait Çetinkaya

My dearies Betül and Şebnem…

ACKNOWLEDGEMENTS

I am deeply indebted to my supervisor **Prof. Dr. Ercan Yılmaz** whose help, stimulating suggestions and encouragement helped me throughout my research and writing of this thesis.

I am dearly obligated to thank my co-supervisor **Assist. Prof. Dr. Aliekber Aktağ** for his valuable helps and advices to complete this research work.

I am especially appreciative to Dr. Russell Duane, Dr. Aleksandar Jaksic, Nikola D. Vasovic and María Sofía Martínez García for their mental and scientific support during my working period in Tyndall National Institute-Ireland.

I would like thank to the SensL Company for the work permit on their new generation silicon photomultipliers. I am very thankful to Tyndall National Institute of University College Cork-IRELAND where I carried out the educational and experimental processes of this thesis.

I would like to thank to the Scientific and Technological Council of Turkey (TUBITAK) for supporting this work under the project number 114F066.

I am appreciative of the aid from Dr. Ayşegül Kahraman, being a great source of help on the issues associated with scintillators. Also, I would like to thank my colleagues Şenol Kaya and Muhammet Turhan for their support.

I would like to thank to International Office of Abant Izzet Baysal University especially the coordinator of Erasmus student mobility program Özlem Yelda Dilmen.

Especially, I would like to give my special thanks to Ferah Özer whose sincere camaraderie made me good since the day we met.

I am very appreciative like a brother of Mehmet İlhan Kutluay for his financial and moral support.

Last but not the least I am heartily grateful to **my family members** who supported and encouraged me a lot during my studies, their prayers and good wishes always accompanied me.

ABSTRACT

INVESTIGATION OF THE SILICON PHOTOMULTIPLIERS SUITABILITY FOR RADIATION DETECTION

CETINKAYA, Ali Osman

Master of Science, Department of Physics

Supervisor: Prof. Dr. Ercan Yilmaz

Co-Supervisor: Assist. Prof. Dr. Aliekber Aktag

January 2015, 65 Pages

Thallium doped Cesium Iodide (CsI(Tl)) scintillator radiation detectors coupled with silicon photomultipliers (SPM) were investigated. The performances of the combinations of CsI(Tl) and SPMs were analyzed in terms of energy calibration, energy resolution, temperature effect and power consumption. The detecting gamma-ray performance of the CsI(Tl)-SPM combinations was discussed and the experimental results were examined by using two different theories. The performance of SPM was compared to traditional photomultiplier tube (PMT) technology in terms of advantages and disadvantages. This study was performed in order to investigate the replacing

potential of PMTs with SPM technology with its reduced size, increased robustness, lower operating voltage and magnetic field sensitivity.

Key Words: Scintillator, Cesium Iodide, CsI(Tl), Silicon Photomultiplier (SPM), Photomultiplier tube (PMT), Dosimetry

ÖZET

RADYASYON TESPİTİNDE SİLİKON FOTOÇOĞALTICILARIN UYGUNLUĞUNUN İNCELENMESİ

ÇETİNKAYA, Ali Osman

Yüksek Lisans, Fizik Bölümü

Tez Danışmanı: Prof. Dr. Ercan Yılmaz

Ortak Tez Danışmanı: Yrd. Doç. Dr. Aliekber Aktağ

Ocak 2015, 65 Sayfa

Silikon fotoçoğaltıcı (SPM) ile birleştilirmiş Talyum katkılı Sezyum İyodür CsI(Tl) sintilasyon radyasyon algılayıcıları incelenmiştir. SPM ve CsI(Tl) birleşimlerinin performansları enerji ölçüm ve ayarları, enerji çözünürlüğü, sıcaklık etkisi ve güç tüketimi açılarından analiz edilmiştir. CsI(Tl) ve SPM kombinasyonlarının gama ışını algılama verimlilikleri tartışılmış ve deneysel sonuçlar iki farklı teori kullanılarak sınanmıştır. SPM' lerin performansları geleneksel fotoçoğaltıcı tüp (PMT) teknolojisi ile avantaj ve dezavantajları bakımlarından karşılaştırılmıştır. Bu çalışma, küçültülmüş boyut, artırılmış sağlamlık, düşük güç tüketimi ve manyetik alan

duyarsızlığı ile SPM teknolojisinin PMT teknolojisinin yerine geçme potansiyelini incelemek üzere yapılmıştır.

Anahtar Kelimeler: Sintilatör, Sezyum İyodür, CsI(Tl), Silicon fotoçoğaltıcı (SPM), Fotoçoğaltıcı tüp (PMT), Dozimetri

TABLE OF CONTENTS

LIST OF FIGURES

LIST OF TABLES

CHAPTER 1

INTRODUCTION

Since nearly 70 years, scintillators belong to the most important nuclear radiation detectors. The detection of ionizing radiation by the scintillation light produced in certain materials is one of the oldest recognized techniques on records. The scintillation process remains one of the most useful methods available for the detection and spectroscopy of a wide assortment of radiations [1]. Scintillators are widely used in the experimental nuclear physics, high-energy physics, nuclear medicine (positron emisssion tomography), environmental studies and many other fields [2]. The basic principle of the scintillation mechanism is that radiation energy is absorbed in the scintillator crystal and then reemitted as photons. The mesurement of the number of the photons emitted from scintillator material is used to obtain the initial radiation dose. Scintillation was started to being used in the beginning of the 20^{th} century with the introduction of the photomultiplier tube (PMT) and it was improved as scintillator counter in the 1940 and 50s [3]. One of the fact that PMT has high quantum efficiency and high amplification, it has been the main choice for photon detection. Lately, however, solid state photodetectors have begun to compete with the PMT with their

higher quantum efficiency in the visible range and above, lower power consumption, smaller size and robustness. The drawback is that the conventional photodiode does not have any internal gain leads to a smaller output signal consequently makes it more sensitive to low level noise [3].

An avalanche photodiode (APD) can be used in order to improve the gain. It has gain in the range of hundreds combined with most of the benefits of the conventional photodiode [3]. The gain depends on the electric field which accelerates the electron. The acceleration gives the electron enough energy to ionize another electron-hole pair when it collides with the crystal lattice. Both these electrons can then accelerate again creating more electron-hole pairs. APDs are very sensitive to changes in temperature and applied bias [1,4]. Geiger-mode avalanche photodiodes (G-APDs) have been developed in recent years and they promise to be an alternative to photomultiplier tubes (PMT). They have many advantages such as single photon response, high detection efficiency, high gain at low bias voltage and very good timing properties but some of their properties, the dark count rate for example, can be a problem. Several types of G-APDs are on the market and should be selected carefully for a given application. APDs are used in Geiger mode in order to get high gain and decrease the sensitivity to temperature [5,6].

Devices which measure the absorbed radiation dose are called as dosimeters. There are two kinds of dosimerters, passive and active. Commonly used passive dosimeters are the Thermo Luminescent Dosimeter (TLD) and the film badge. Active dosimeters give real time response to the radiation, typically an electronic personal dosimeter (EPD). For real time measurements, the response time is also of importance [3].

Silicon photomultiplier (SPM) based scintillator radiation detectors have been used in many applications, especially in nuclear medicine and homeland security operations. Silicon photomultiplier is a constantly being developed new solid state photodiode technology which has the capability of replacing traditional photomultiplier technology with advantages such as reduced size, increased robustness, lower operation voltage and magnetic field insensitivity [7,8]. In this study, we focus on the response of large arrays of silicon photomultipliers developed by Sensl technologies for detection of radiation. We compare experimental results with two different theories. Experimental results are in good agreement with theoretical results and these agreements show that large silicon photomultiplier arrays are interesting candidate for detection of gamma radiation. The purpose of this thesis is to investigate the possibility of using the combination of SPM and scintillator materials to detect low dose gamma radiation on a wide spectrum.

To investigate the properties of CsI(Tl) combined with SPMs to detect low dose rates and to do dosimetry on a wide energy spectrum, a measuring set up was constructed. The data were analyzed by using efficiency calculations.

CHAPTER 2

THEORETICAL BACKGROUND

2.1 Energy Absorbtion in Matter

Photons are electromagnetic radiation having zero mass, zero charge, and speed ***c*** which is the the speed of light. Because they are electrically neutral, they do not steadily lose energy via coulombic interactions with atomic electrons, as do charged particles. Photons travel some considerable distance before undergoing a more "catastrophic" interaction leading to partial or total transfer of the photon energy to electron energy. These electrons will ultimately deposit their energy in the medium. Photons are far more penetrating than charged particles of the same energy. Although a large number of possible interaction mechanisms are known for gamma rays in matter, only three major types play an important role in radiation measurements: photoelectric absorption, Compton scattering, and pair production. All these processes lead to the partial or complete transfer of the gamma-ray photon energy to electron energy. They result in sudden and abrupt changes in the gamma-ray photon history, in that the photon

either disappears entirely or is scattered through a significant angle [1,3,9]. In this section, we will describe each one briefly.

2.1.1 Compton Scatttering

The interaction process of Compton scattering takes place between the incident gamma-ray photon and an electron in the absorbing material. It is most often the predominant interaction mechanism for gamma-ray energies typical of radioisotope sources.

In Compton scattering, the incoming gamma-ray photon is deflected through an angle θ with respect to its original direction. The photon transfers a portion of its energy to the electron (assumed to be initially at rest), which is then known as a recoil electron. Because all angles of scattering are possible, the energy transferred to the electron can vary from zero to a large fraction of the gamma-ray [1]. The expression that relates the energy transfer and the scattering angle for any given interaction can simply be derived by writing simultaneous equations for the conservation of energy and momentum. The mechanism of the photoelectric effect can be seen in **Figure 2.1.**

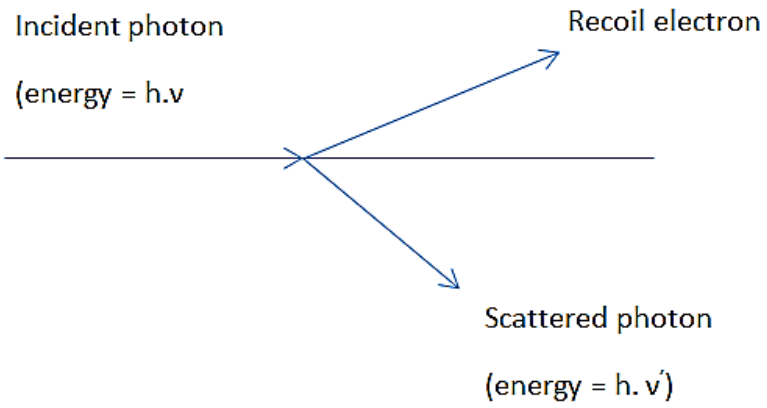

Figure 2.1: The Compton scattering mechanism.

The Compton effect involves scattering in high energy photons off of electrons and observing the shift in wavelength between the incident and the scattered photons. Compton theorized that if photons carry energy, they should also carry momentum. The energy (E) of a particle is related to its mass (m) and momentum (p),

$$E^2 = (pc)^2 + (mc^2)^2 \qquad (2.1)$$

where c is the speed of light. Since the mass of a photon is zero, its energy becames $E = pc$. The energy may also be defined as $E = hv$, where h is Planck's constant and v is frequency. Using these relations, the momentum of a photon is related to its wavelength (λ), $p = h / \lambda$. Compton argued that the shift in wavelength is a result of a single photon imparting momentum to a single electron. Therefore, the theory is derived from the laws of conservation of energy and momentum [10].

Consider a photon with energy E_0 and momentum p_0, and a stationary electron with rest energy mc^2. When the photon collides with the electron, the electron recoils

with energy E_e and momentum p_e. The scattered photon will have an energy E and momentum p. By conservation of energy and momentum,

$$E_e + E = mc^2 + E_0 \tag{2.2}$$

and

$$p_e + p = p_0 \tag{2.3}$$

combining energy and momentum conservation and using equation (2.4) yields,

$$\lambda - \lambda_0 = \frac{h}{mc(1 - cos\theta)} \tag{2.4}$$

The shift in the wavelength is related only to the mass of the electron and the backscattered angle. The shift has no relation with the energy of the incident photon. The Compton effect can also be expressed as a shift in energy between the incident and scattered photon [10].

$$E - E_0 = \frac{E_0 E}{(mc^2)(1 - cos\theta)} \tag{2.5}$$

For a 180° C backscattered photon, the shift in energy between E_0 and E is

$$E_0 - E = E_0 \left(\frac{2E_0}{2E_0 + mc^2}\right) \tag{2.6}$$

2.1.2 Photoelectric Effect

For all the energy in the incident photon to be absorbed, the electron has to be bound to the atom. When the electron hit, it is ejected from the atom and is then called a photoelectron. In the photoelectric absorption process, a photon undergoes an interaction with an absorber atom in which the photon completely disappears. In its place, an energetic photoelectron is ejected by the atom from one of its bound shells.

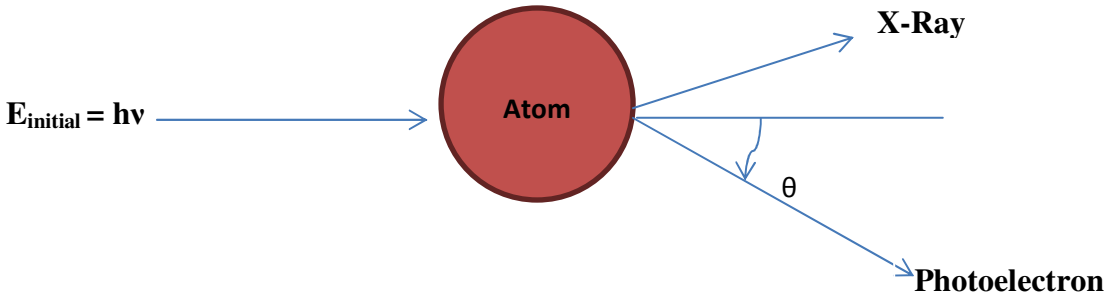

Figure 2. 2: Photoelectric effect mechanism.

The interaction between the atom and the photon as a whole and cannot take place with free electrons. For gamma rays of sufficient energy, the most probable origin of the photoelectron is the most tightly bound or K shell of the atom. The energy of the photoelectron is given by equation

$$E_{e^-} = h\nu - E_b \tag{2.7}$$

where $h\nu$ is the energy of the incident photon and E_b is the binding energyof the electron. When the vacancy from the photoelectron is filled, characteristic X-rays or Auger electrons are created. The Auger electron is always reabsorbed but the characteristic X-ray can escape without further interaction in the absorber material. For gamma-ray energies of more than a few hundred keV, the photoelectron carries off the majority of the original photon energy.

The photoelectric process is the predominant mode of interaction for gamma rays (or X-rays) of relatively low energy. The process is also enhanced for absorber materials of high atomic number Z. No single analytic expression is valid for the probability of photoelectric absorption per atom over all ranges of $E\gamma$and Z, but a rough approximation is

$$[\cong constant \times Z^n/(E_\gamma^{3.5}) \quad (2.8)$$

where the exponent n varies between 4 and 5 over the gamma-ray energy region of interest. This severe dependence of the photoelectric absorption probability on the atomic number of the absorber is a primary reason for the preponderance of high-Z materials (such as lead) in gamma-ray shields [1].

2.1.3 Pair Production

If the gamma-ray energy exceeds twice the rest-mass energy of an electron (1.02 MeV), the process of pair production is energetically possible. As a practical matter, the probability of this interaction remains very low until the gamma-ray energy approaches several MeV and therefore pair production is predominantly confined to high-energy gamma rays. In the interaction (which must take place in the coulomb field of a nucleus), the gamma-ray photon disappears and is replaced by an electron-positron pair. All the excess energy carried in by the photon above the 1.02 MeV required to create the pair goes into kinetic energy shared by the positron and the electron [1].

If the incident photons' energy exceeds (the mass of the electron + the positron) pair production becomes possible. The photon is then completely absorbed and an electron-positron pair is created, its kinetic energy is given by equation [3].

$$T_{pp} = E - 2m_0 c^2 \quad (2.9)$$

The positron and the electron will slow down in the absorbing medium and deposit all its kinetic energy. The positron will then interact with an electron resulting in two annihilation photons at energies of 511 keV. These can either be absorbed by Compton scattering or the photoelectric effects, or one or both can escape. The resulting energy, if both photons escape, is called the "double escape peak" and is consequently located at $h\nu - 2m_0 c^2$. If only one photon escapes the "single escape peak" is located at $h\nu - m_0 c^2$. The probability of pair production increases with high energies and does not give any effect before the energy is several MeV, then the pair production impact rises sharply. The dependence of the absorber material can be approximated as the square of the atomic number [3].

2.2 Overview to Scintillation

Scintillation is a general term referring to the process of giving off light; it is used both literally and figuratively. More specifically in sciences, a scintillator is any material that can release a photon in the UV or visible light range, when an excited electron in the scintillator returns to its ground state. These scintillation photons are detected by a photomultiplier and converted into an electronic signal.

2.3 Radiation Interaction with Scintillators

Scintillators can be fabricated in different sizes. The thickness of the scintillator is important and it determines the ability to absorb and detect certain radiation

emissions. Generally, a thin scintillator is an excellent choice for low-energy gamma rays. The ray or particle will be absorbed within the thin scintillator and the light produced by this interaction will be able to pass through the remaining thickness to allow the gamma ray to be detected. A high-energy gamma ray is likely to pass right through the thin scintillator without interacting.

The best choise for the radionuclides emitting high-energy gamma rays is a thick scintillator. A thick scintillator is the choice for radionuclides emitting high-energy gamma rays. The scintillator must be thick enough to absorb the gamma ray but not too thick to prevent the light that is produced from being detected. A thick scintillator is not very good for detecting low-energy gamma rays; they interact but if the scintillator is too thick, it absorbs the light that is produced before it can be detected.

2.4 Scintillation Mechanisms in Different Types of Scintillators

Many kind of materials have the ability of scintillate. Organic materials, particularly conjugated ring compounds, produce scintillation photons in the process of de-excitation of orbital electrons. Scintillators can also be made of glass or of noble gases such as xenon or helium, both of which may be used for detection of particulate radiation. However, all these scintillators have a low atomic number, and therefore are not very good efficient for interactions with gamma rays.

The scintillators used in nuclear medicine applications are inorganic crystalline scintillators, often with small amounts of impurities that help them scintillate more efficiently.

The ideal scintillation material should possess the following properties:

- It should convert the kinetic energy of charged particles into detectable light with a high scintillation efficiency.
- This conversion should be linear, the light yield should be proportional to deposited energy over as wide range as possible.
- The medium should be transparent to the wavelength of its own emission for good light collection.
- The decay time of the induced luminescence should be short so that fast signal pulses can be generated.
- The material should be of good optical quality and subject to manufacture in sizes large enough to be of interest as a practical detector.
- Its index of refraction should be near that of glass (-1.5) to permit efficient coupling of the scintillation light to a photomultiplier tube or other light sensor [1].

Following two parts will give information about two main scintillator types and their principles of scintillation.

2.4.1 Scintillation Mechanism in Organic Scintillators

Organic scintillators (plastics, liquids), on the contrary, are composed of aromatic hydrocarbons. Plastic scintillators are non-fluid solutions consisting of fluorescent compounds dissolved in a solidified polymer matrix. Liquid scintillators are fluid solutions with similar fluorescent organic compounds. Unlike inorganic

scintillators, organic scintillators scintillate on a molecular level. Basically, each scintillator molecule can act as a scintillator center.

In an organic molecule the light emission emerges from the transitions between different energy levels. When a charged particle, passing by its kinetic energy, is absorbed by the molecule causing it to excite to a higher energy state. If the molecule is excited to the vibrational state surrounding a higher state it is also quickly returned to the ground state since the vibrational states are not at thermal equilibrium. This process is fast compared to the inorganics with typical decay times in the size of a couple of nanoseconds. Some molecules can cross over to the triplet states, the decay time here is much longer than for the singlet states and the wavelength is longer since the energy gap is small. The de-excitation from these states gives rise to phosphorescence. Since almost all the fluorescence is emitted at a shorter wavelength than the absorption the self absorption is small [1].

2.4.2 Scintillation Mechanism in Inorganic Scintillators

The scintillation mechanism in inorganic materials depends on the energy states determined by the crystal lattice of the material. The valence and the conduction bands are separated by a forbidden band where no electrons can be found. A perfect crystal lattice will have a large band gap and the amount of charge carriers will be negligible at normal temperatures. However, if an electron is excited to the conduction band the de-excitation will be an inefficient process and the wavelength will be too small to be in the range of visible light.

To get a good light yield from these scintillators, an impurity is added, called activator. The activator creates sites in the forbidden gap where de-excitation can occur. This makes the band gap smaller and the emitted photons will be in the visible range. As a charged particle pass through the crystal, electrons will be excited from the valence band to the conduction band. This creates electron-hole pairs and the holes will find an activator site to ionize. When an electron finds an activator site, it might recombine and de-excite to the ground state. This requires that the transition is allowed and will then result in photon emission which is very likely to be in the visible range [1,3].

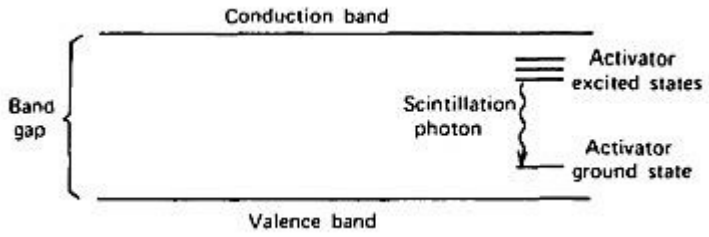

Figure 2. 3: Energy band structure of an activated crystalline scintillator [1].

In the conversion to scintillation light there also exists some lose mechanisms called quenching, this is when the excitation energy is dissipated by radiationless thermal transitions. The quenching processes give rise to the nonlinearity that can be observed in inorganic scintillators, the nonlinearity is, however, much less than in the organics.

Since the energy needed to create the initial electron hole pairs is larger than the impurity emission the crystal lattice is transparent to this which makes self absorption

negligible. For pure crystal scintillators this effect is significant and limits their use to small sizes [3].

2.5 Photomultipliers

The widespread use of scintillation counting in radiation detection and spectroscopy would be impossible without the availability of devices to convert the extremely weak light output of a scintillation pulse into a corresponding electrical signal. The photomultiplier tube (PMT) accomplishes this task remarkably well, converting light signals that typically consist of no more than a few hundred photons into a usable current pulse without adding a large amount of random noise to the signal. And the new silicon photomultiplier (SPM) is a constantly being developed new solid state photodiode technology which has the capability of replacing traditional photomultiplier technology with advantages such as reduced size, increased robustness, lower operation voltage and magnetic field insensitivity [1,11].

2.5.1 Photomultiplier Tube Mechanism

A PMT is a vacuum tube consisting of an input window, a photocathode, focusing electrodes an electron multiplier and an anode usually sealed into an evacuated glass tube. **Figure 2.4** shows the schematic construction of a photomultiplier tube [1].

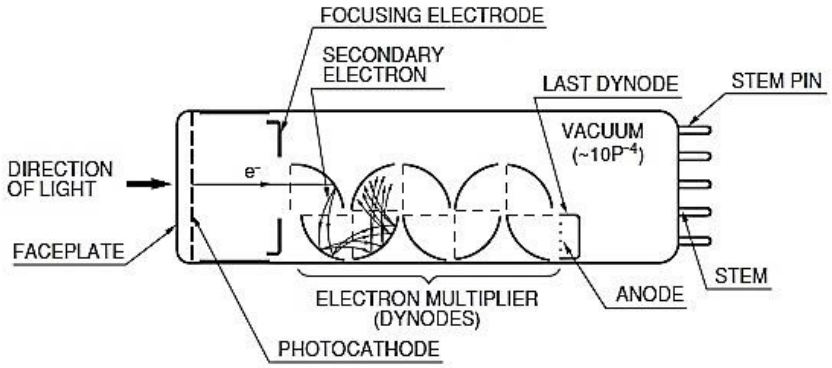

Figure 2. 4: Construction of a photomultiplier tube [12].

Light which enters into the PMT is detected and produces an output signal. The produced light passes through the input window and excites the electrons in the photocathode so that photoelectrons are emitted into the vacuum. The photoelectrons are accelerated and focused by the focusing electrode onto the first dynode where they are multiplied by means of secondary electron emission. This secondary emission is repeated at each of the successive dynodes. At the end of the process, the multiplied secondary electrons emitted from the last dynode are finally collected by the anode [12]. Typical operating voltages of PMTs are in the range of 500 to 3000 V [12]. PMT is affected by electromagnetic fields. A unit of bigger significance in scintillation counting is the quantum efficiency (QE) for the photomultiplier. The quantum efficiency can be defined as

$$QE = \frac{number\ of\ photoelectrons\ \ emitted}{number\ of\ incident\ photons} \tag{2.10}$$

PMTs are the most common light amplifiers used with scintillators, both in pulse and current mode operation. However, advances in the development of semiconductor

photodiodes (SPM) have led to the substitution of solid-state devices for PMTs in some applications. In general, photodiodes offer the advantages of higher quantum efficiency, lower power consumption, more compact size, and improved ruggedness compared with PMTs used in scintillation counting. SPMs are also virtually insensitive to magnetic fields and therefore can sometimes be substituted in experiments where magnetic fields prevent the use of PMTs. Because of the relatively small dimensions over which charges must move in these devices, their time response is comparable to that of conventional PMTs, and they can be used for coincidence and other timing applications [1,13].

2.5.2 Silicon Photomultipliers

The silicon photomultiplier (SPM) was developed in Russia in the mid 1980s and it uses an array of avalanche photodiodes (APDs) to get a good sensitivity for small numbers of photons[3]. While the nomencleature for the SPMs/APDs is not unambiguous in the many studies/literatures, many different terms can be found to describe the same type of device (SiPM, MPPC, SPM, PPD, APD) [14,15]. In the avalanche photo diodes the same thing happens as in the ordinary photodiode but in the APD there is a high electrical field which accelerates the electron when it enters this region[3]. The SPM is a semiconductor device consisting of many photon microcounters positioned on a common Si substrate. It is a multipixel silicon photodiode with a number of micropixels [16]. The acceleration gives the electron enough energy to ionize another electron-hole pair when it collides with the crystal lattice. Both these electrons can then accelerate again creating more electron-hole pairs. This gives an internal gain to the diode typically in the size of hundreds[3].

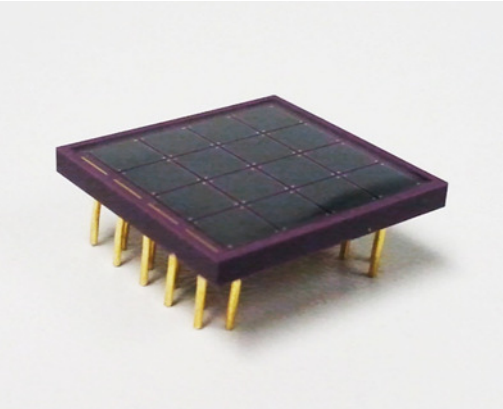

Figure 2. 5: A picture of silicon photomultiplier (SPM).

In recent years, SPMs have emerged as a promising light sensor for compact, low-bias scintillation detectors. They have a gain comparable to that of the typical PMT while offering a number of key advantages compared to the latter such as **compactness, operation at low bias voltage, robustness, insensitivity to magnetic fields, and in some cases, fast timing** properties. In addition, operation under ambient light, while not recommended for optimum noise levels, will not cause permanent damage to the SPM. Sizes are increasing as smaller individual sensors are tiled together [15]. The SPM has gain and timing resolution comparable to that of a PMT, requiring a simple electronic circuit and is not sensitive to magnetic fields [17,18].

Table 2.1: Comparing of SMP with PIN, APD and PMT technologies.

	PIN	APD	PMT	SPM
Gain	1	10^2	10^6	10^6
Operational Bias	Low	High	High	Low
Temperature sensitivity	Low	High	Low	Low
Mechanical Robustness	High	Medium	Low	High
Ambient Light Exposure	OK	OK	No	OK
Read-out electronics	Complex	Complex	Simple	Simple
Form-factor	Compact	Compact	Bulky	Compact
Large area available	No	No	Yes	Yes
Sensitive to magnetic fields	Yes	Yes	Yes	No
Noise	Low	Medium	Low	High
Rise time	Medium	Slow	Fast	Fast

Many investigations have been made on the SPM technology and a number of publications have followed since on its various possible applications ranging from the general subject of radiation detection to more specific applications such as medical imaging, basic research in physics, low-intensity light biosensors, and laser radar systems [1,5,15,19].

2.5.2.1 Overview to Silicon Photomultipliers

The SPM addresses the challenge of detecting, timing and quantifying low light signals down to the single photon level. The SPM offers low voltage operation,

insensitivity to magnetic fields, mechanical robustness and excellent uniformity of response. Due to these traits, the SPM has rapidly gained a proven performance in the fields of medical imaging, hazard and threat detection, biophotonics, high energy physics [20].

When a photon propagates through silicon, it can transfer its energy to a bound state (valence) band, thereby transporting it into the conduction band, creating an electron-hole pair. The absorption length of a photon in silicon depends on its energy. This illustrates that silicon is a good photo detector material in the spectral range from 350nm up to 800nm. Above 1000nm, the absorption length becomes so large that a silicon based detector becomes too bulky, and below 350 nm, too thin.

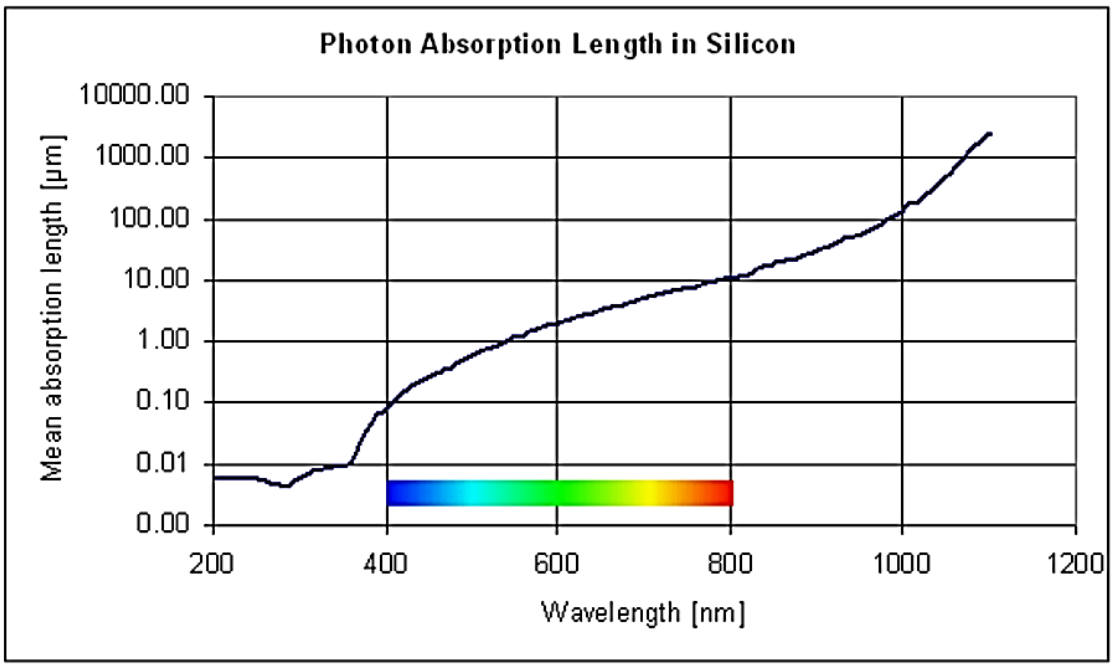

Figure 2. 6: Photoelectric absorbtion lenght in Silicon [20].

The photon absorbtion of a SPM is exploited to detect incident light. Applying a reverse bias to a diode will counteract the diffusive force that draws negative and positive charge carriers to the depletion region situated around the p-n junction. Under application of the reverse bias, an absorbed photon will result in a net current electrons through the n-type and holes through the p-type sides of the device [20].

When a sufficiently high electric field generated within the depletion region of the silicon higher than $5x10^5$ (V/cm), a charge carrier created in this region will be accelerated to a point where it carries sufficient kinetic energy to create secondary charge pairs through a process called impact ionization. In this way, a single photoelectron can trigger an self-perpetuating ionization cascade that will be spreaded throughout the silicon volume subjected to the field. The silicon will break down and become conductive, effectively amplifying the original photoelectron into a macroscopic current flow. This process is called Geiger discharge. A SPM is operated in Geiger mode employs this mechanism of breakdown to achieve a high gain. The p-n junction region is fabricated in such a way to sustain a reverse bias beyond its nominal breakdown voltage, creating the necessary high field gradients across the junction [20].

Each photodiode component on the SPM is called as a microcell. Typically numbering between 100 and 1000 per mm^2, each microcell has its own quenching resistor. The signals of all microcells are then summed to form the output of the SPM. Each microcell detects photons identically and independently. The sum of the discharge currents from each of these individual binary detectors combines to form a quasi-anlog output, and is thus capable of giving information on the magnitude of an incident photon flux [20].

2.5.2.2 Optimum Silicon Photomultiplier (SPM) Specialities for Scintillation Radiation Detector

The SPM is a novel and rapidly developing solid-state optical sensor. Its low power consumption, small dimensions, and high gain make SPM of great interest for applications in portable radiation detection instrumentation based on scintillation materials. In contradistinction to its use for photon counting, the operating conditions of SPM are of primary concern when it is used as a light sensor in radiation detection due to the gain dependence on temperature and operating voltage. The improvement and optimization of these operational considerations directly affect the critical parameters and the performance of radiation detectors. For instance, the photon detection efficiency (PDE) of SPM directly influences the signal-to-noise ratio (SNR) and thus the significant parameters for isotope identification, such as the full-width at half-maximum (FWHM). Optimization of PDE can be achieved by increasing the pixel size, thereby improving the detector geometrical fill-factor (FF) and the sensitive area. Conversely, this increase in pixel size reduces the number of pixels [21].

The users of SPM detectors will typically be interested in the following parameters: gain, PDE, noise, dynamic range, timing and temperature sensitivity [20]. Each microcell in a SPM is comprised of a Geiger-mode photodiode in series with an integrated quench resistor. Each microcell generates a highly uniform and quantized amount of charge every time the microcell undergoes a Geiger breakdown. The gain of a microcell is defined as the ratio of the output charge to the charge on an electron.

The PDE of an SPM is the statistical probability that an incident photon will produce a Geiger pulse from one of the SPM microcells. It differs slightly from the

quantum efficiency (QE) that is quoted for a PMT or APD, due to the microcell structure of the device [20].

2.6 Gamma Radiation Detectors based on Cesium Iodide CsI(Tl) Scintillators

Scintillation detectors are used when high sensitivity is required. So that many applications need scintillation detection systems [22]. A scintillator is a material that converts radiation energy into pulses of light. Those pulses of light emitted by the scintillation material can be detected using a sensitive light detector. In a scintillation detector, this emitted light is collected and measured to provide an indication of the amount of incident radiation. Scintillation materials have different characteristics. They are distinguished by **density, sensitivity, temperature dependence, emission light output spectra, decay time, and mechanical and optical properties** [21].

2.6.1 Scintillation Properties of Cesium Iodide CsI(Tl)

In general, the two main parameters had preponderance over all the rest: cost effectiveness and compatibility with a solid-state photo-sensor. The CsI(Tl) crystal was superior in both. Though NaI(Tl) is widely used and known as the traditional choice for scintillation radiation detectors, CsI(Tl)s wavelength compatibility is best suited for silicon solid-state photo-detectors [21].

CsI(Tl) is another alkali halide that has gained substantial popularity as a scintillation material. It is commercially available with either thallium or sodium as the activator element, and very different scintillator properties are produced in the two

cases. CsI(Tl) has a somewhat larger gamma-ray absorption coefficient per unit size compared to sodium iodide. This advantage is of primary importance for applications such as space instrumentation where size and weight are at a premium. Because it is less brittle than sodium iodide, it can be subjected to more severe conditions of shock and vibration. When cut into thin sheets, cesium iodide may be bent into various shapes without fracturing, and it is reasonably soft and malleable [1].

2.6.2 Light Output, Energy Resolution and Decay Time of Cesium Iodide CsI(Tl)

The emission spectrum of CsI(Tl) is peaked at a much longer wavelength than that for NaI(T1) and is poorly matched to the response of PMT. For that reason, the light output is often quoted as being substantially lower in CsI(T1). However, when measurements are made using SPMs with extended response into the red region of the spectrum, the scintillation yield is actually higher than that of any other scintillator. The absolute light yield at room temperature is measured to be about 65,000 photons/MeV, with a maximum value about 6% higher at -35°C. The yield falls off with temperature change on either side of this maximum, to 64% of the room temperature value at -100°C and to 95% at +50°C [1].

A most useful property of CsI(Tl) is its variable decay time for various exciting particles. Pulse shape discrimination techniques can therefore be used to differentiate among various types of radiation. Particularly clean separations can be achieved between charged particles such as protons or alpha particles on one hand-and electron events on the other hand. CsI(Tl) is less hygroscopic than NaI(T1) but will deteriorate if exposed to water or high humidity [1].

CHAPTER 3

THE METHOD OF ANALYZING OF DATA AND COMPARING WITH THE THEORY

3.1 Detector efficiency

The detector counting efficiency (***DE***) relates the amount of electromagnetic radiation emitted by a radioactive source to the amount measured by the detector. The ***DE*** can be used to calculate the counting rate expected in a detector when the source strength is known or to calculate the source strength by measuring the counting rate in the detector. The ***DE*** is the ratio of the measured counting rate (total events in a known time interval) to the counting rate (or total events) emitted by the radiation source.

$$DE = \frac{D}{N} \tag{3.1}$$

where ;

DE= detector efficiency,

D= the number of photons counted in the detector,

N= number of photons emitted by the source [23].

The detector efficiency of a scintillator depends upon the density of electrons in the detector crystal such as sodium iodide NaI, cesium iodide CsI(Tl) and bismuth germanate (BGO) achieve high electron densities as a result of the high atomic numbers of the elements of which they are composed. The detector efficiency of scintillators is also a function of gamma-ray energy used as a radiation source [24].

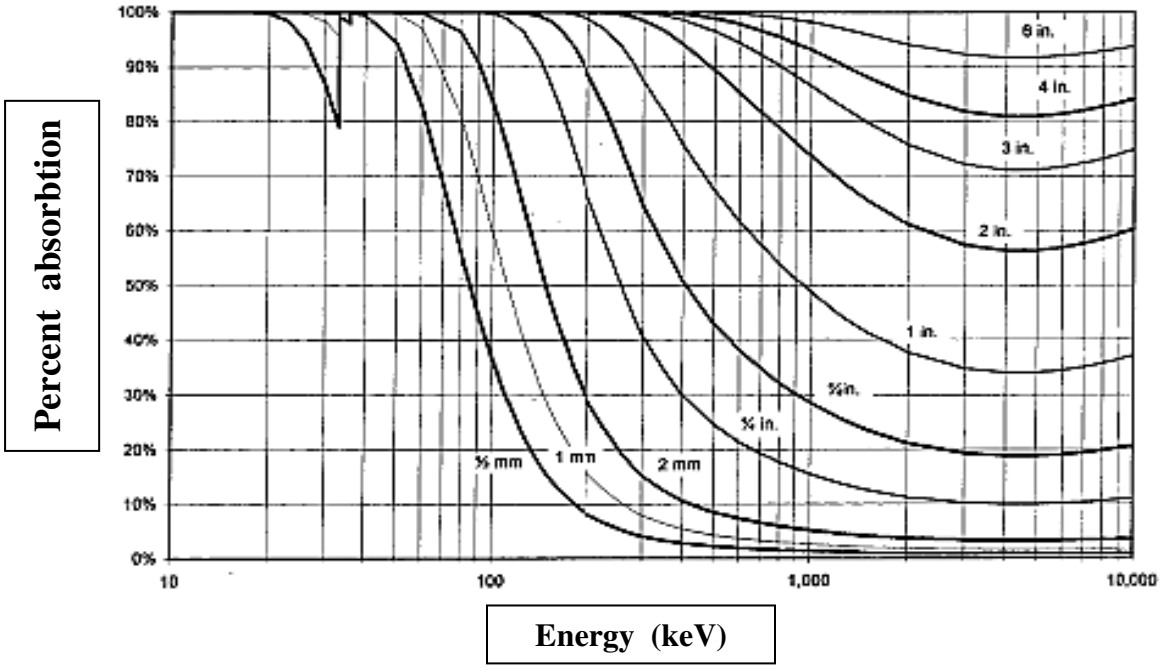

Figure 3. 1: Absorbtion efficiency of CsI(Tl) scintillator detector [23].

Figure 3.1 shows the energy absorbtion yield of CsI(Tl) scintillators for certain values of t. The number of photons absorbed by a certain thickness is the difference $I_0 - I$. However, instead of calculating I for different I_0's the ratio called the "percent absorption", $\frac{I_0 - I}{I_0}$ values were calculated [23].

3.2 Calculating number of photons emitted by the source (*N*):

The activity of a radioactive source is usually given in Curies (abbreviated ***Ci***). One ***Ci*** is defined to be **3.7 x 10^{10}** disintegrations per second (***dps***):

$$1\ Ci = 3.7 \times 10^{10} dps \tag{3.2}$$

N can be calculated from the activity ***A*** by multiplying by the branching fraction ***BF*** for that mode of decay and the branching ratio ***BR*** for that photon energy and the counting time interval ***T***. (Sometimes the total branching ratio ***TB***, which is the product of ***BF*** and ***BR***.)

$$N = BF \times BR \times T \times A \tag{3.3}$$

or

$$N = TB \times T \times A \tag{3.4}$$

where,

BF = the branching fraction for that mode of decay,

BR = the branching ratio for that photon energy,

TB = total branching ratio **(TB = BF x BR),**

T = the total counting time interval in seconds,

A = the activity in dps [23].

3.3 Branching Ratio

Each radioactive material has a characteristic branching ratio. This concept can be determined as the separation of the rays when they are travelling in the space or in a

medium. Especially in radiation detection systems, the branching ratio of the radiation source must be determined in order to make a correct comparing with the theory.

Table 3.1: Branching ratios of some radioactive materials.

Radoactive Source	E (keV)	Total Branching Ratio (TB)
Am-241	59.5	0.36
Co-60	1173	1.00
Co-60	1332	1.00
Co-60	1173&1332	2.00
Cs-137	662	0.85
Ba-133	356	1.00
Ge-68	511	1.8

3.4 Solid Angle (*G*):

Solid angle is the concept of fraction of all space that the detector subtends. Unless the detector completely surrounds the source, the geometrical solid angle factor is less than 1.

$$G = \frac{Area}{4\pi r^2} \tag{3.5}$$

where,

Area: area of detector face,

$4\pi r^2$: area of sphere with a radius equal to the source to detector distance [23].

3.5 Peak to Total Ratio (Theory 1):

For low energy photons, those that are absorbed as a photoelectric event in the detector, ***D*** is the net counts in the photopeak for that energy. Above 100 keV, Compton events become appreciable and, above 2 MeV, pair production events become appreciable. For these higher energy cases, it is necessary to know the fraction of events in the photopeak or the peak-to-total ratio ***R*** so that the net counts in the photopeak ***P*** can be related to the total counts in the detector.

In many applications, it is desirable to discriminate against background radiation. In these instances, it is necessary to count only the full energy or photopeak events generated by a detector. So that, the background counts must be subtracted from the total spectrum.

There is no easy way to calculate the number of events that are expected in the photopeak only. The absorbtion efficiency of CsI(Tl), as shown in **figure 3.1**, gives the total counts (***D***) that can be expected in the channel or energy integrated spectrum. However, this includes the full energy peak, Compton edge, single and double escape peaks, backscattered and other Compton events. To get the number of events in the photopeak (***P***) only, the absorbtion efficiency should be multiplied by the photofraction

(***R***), also called the peak-to-total ratio. These quantities are related by the following equation:

$$P = \frac{R}{D} \tag{3.6}$$

The photofractions or photopeak efficiency for various geometries of CsI(Tl) detectors are shown in **figure 3.2.** These were calculated using a Monte Carlo method [23].

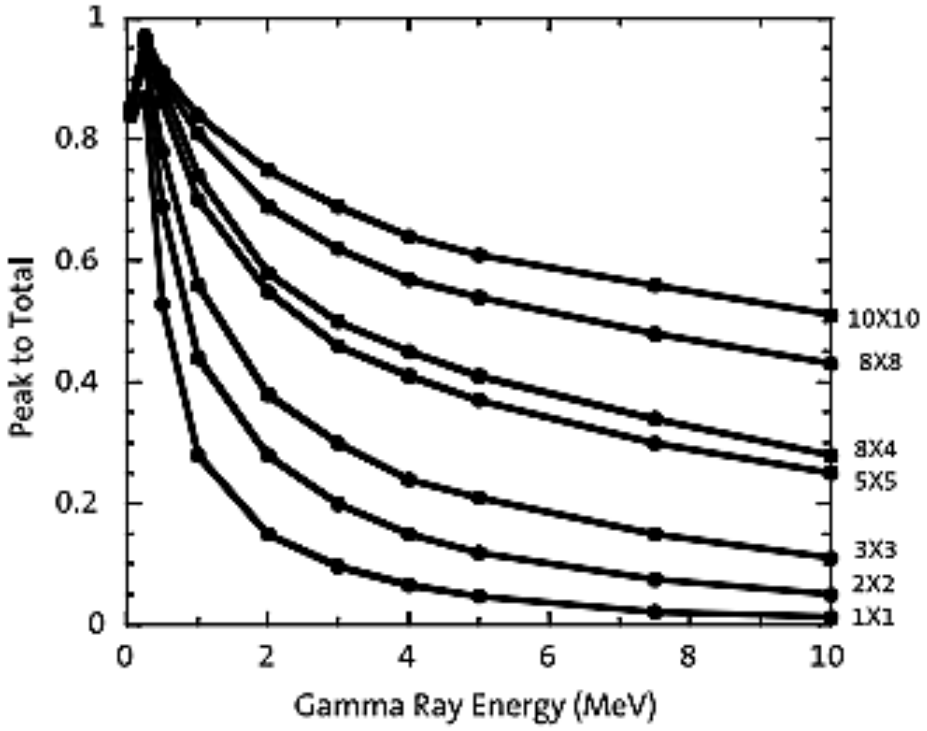

Figure 3.2: Peak-to-total ratio graph for different dimensions of CsI scintillator from 0 MeV to 10 MeV gamma energies [23].

According to theory 1 for the calculation of peak to total ratio, the mathematical relationship between the amount of radiation emitted and that absorbed by a detector has

been discussed. If the above equations combined, the counting rate expected in a photopeak from a known source in a known geometry can be estimated;

$$P = DE \times R \times BF \times BR \times T \times A \tag{3.7}$$

where,

P= the number of counts in the photopeak,

DE = the detector efficiency,

R = the peak-to-total ratio,

BF = the branching ratio for that photon energy,

T = total counting time interval in seconds,

A = the activity of the source in disintegrations per seconds (dps, corrected for decay) [23].

3.6 Mass Attenuation Coefficient and Absorber Mass Thickness (Theory 2):

Each of the interaction processes removes the gamma-ray photon from the beam either by absorbtion or by scattering away from the detector direction and can be characterized by a fixed probability of occurrence per unit path length in the absorber [25]. The sum of these probabilities is simply the probability per unit path length that the gamma-ray photon is removed from the beam:

$$\mu = (\tau)photoelectric + (\sigma)Compton + (\kappa)pair\ production \tag{3.8}$$

and is called the linear attenuation coefficient. The number of transmitted photons I is then given in terms of the number without an absorber I_0 as;

$$\frac{I}{I_0} = e^{-\mu t} \tag{3.9}$$

Use of the linear absorbtion coefficient is limited by the fact that it varies with the density of the absorber, even though the absorber material is the same. Therefore, the mass attenuation coefficient is much more widely used and is defined as;

$$mass\ attenuation\ coefficient = \frac{\mu}{\rho} \tag{3.10}$$

In terms of the mass attenuation coefficient, the attenuation law for gamma rays now takes the form,

$$I = I_0 e^{-\left(\frac{\mu}{\rho}\right)\rho t} \tag{3.11}$$

where,

I : the number of photons that have passed through a layer of thickness t,

I_0 : the number of photons of a certain energy incident or entering the slab of material,

μ/ρ : mass attenuation coefficient,

t : thickness of the absorber.

The product ρt, known as the mass thickness of the absorber, is now the significant parameter that determines its degree of attenuation. Units of mass thickness have historically been mg/cm^2. The thickness of absorbers used in radiation measurements is therefore often measured in mass thickness rather than physical thickness, because it is a more fundamental physical quantity.

The mass thickness is also a useful concept when discussing the energy loss of charged particles and fast electrons. For absorber materials with similar neutron/proton ratios, a particle will encounter about the same number of electrons passing through absorbers of equal mass thickness. Therefore, the stopping power and range, when expressed in units of ρt, are roughly the same for materials that to not differ greatly in Z [1].

So that; in this theory we can calculate the total counted photons in a scintillator detector as;

$$N = A \times BR \times \left(\frac{1}{I/I_0}\right) \times G \tag{3.12}$$

where;

N = total counts per seconds,

BR = the branching ratio for that photon energy,

A = the activity in dps,

G = solid angle,

$\frac{1}{I/I_0}$ = detector efficiency.

3.7 Peak to Total Ratio (Theory 2):

The full energy peak (*FEP*) efficiency of a gamma-ray detector, ε_p , can be expressed by the product $\varepsilon_p = \varepsilon_T \times P/T$ where ε_T is the total efficiency, i.e. the primary interaction probability of a photon with the detector, and P/T, the peak-to-total ratio, is the probability that the photon energy be entirely absorbed in it . The P/T value depends on the photon energy, the detector dimensions and the material which fills the active volume, but it does not depend appreciably on the source to detector distance or on the source shape, so that, at each energy, this quantity is characteristic of a given detector [26].

Cesena et al. showed that the peak to tatal ratio for scintillator crystals can be calculated to a very good approximation by means of the simple expression:

$$P/T = 1 - a(E)\exp\left[-b(E)\frac{V}{A}\right] \qquad (3.13)$$

where *V/A* is the detector volume-to-surface ratio. The coefficients ***a(E)*** and ***b(E)*** depend only on the photon energy; they were empirically determined by using a set of experimental data covering the whole range of heights and radii of practical interest [26].

The procedure for peak-to-total ratio evaluation is straightforward .Once the $b_r(E)$ value at a given energy for a reference material is known, the P/T value at the same energy for any material is obtained by the equation;

$$P/T = 1 - \left(1 - \tau/\mu\right)\exp\left[-\frac{b_r(E)RV}{A}\right] \qquad (3.14)$$

where,

P/T = peak to total ratio.

The values of ***b(E)*** were given in **Table 3.2**. Although the variances are relatively high these results suggest that the ***b(E)*** functions have the same energy dependence so they can all be written in the form $Rb_r(E)$, where ***R*** is a constant that depends on the detector material and ***r*** indicates a reference material. Using the data of **Table 3.2** and Ge as reference material, the following mean values of ***R*** are obtained for CsI(Tl). [26].

$R_{CsI}=b_{CsI}/b_{Ge}$= 2.980.19.

Table 3.2: The empirical values of *b(E)* [cm^{-1}] [26].

Energy (MeV)	b_{Ge}	b_{NaI}	b_{CsI}	b_{BGO}
0.3	0.40±0.12	0.90±0.13	1.3±0.0.10	-
0.4	0.34±0.07	0.74±0.09	1±0.10	-
0.5	0.29±0.05	0.57±0.05	0.86±0.07	-
0.8	0.22±0.04	0.43±0.03	0.59±0.03	2.4±0.2
1	0.18±0.03	0.37±0.03	0.50±0.03	1.6±0.3
1.5	0.12±0.03	0.26±0.01	0.37±0.02	1±0.1
2	0.10±0.01	0.21±0.01	0.30±0.01	0.82±0.1
3	0.076±0.008	0.17±0.01	0.24±0.01	0.59±0.04
4	0.049±0.009	-	-	0.46±0.04
6	0.024±0.007	-	-	0.31±0.06

Table 3.3: Values of the parameter $a(E) = 1 - {}^{\tau}/\mu$ vs energy for some detectors and of the parameter $b_r(E)$ **[cm^{-1}]** for the Ge (reference) detector. Values of $b(E)$ for other detectors can be obtained by multiplying by the appropriate **R** factor [26].

Energy (MeV)	Ge (R=1) a(E)^b	br(E)	NaI (R=2.03) a(E)^b	CsI (R=3.07) a(E)	BGO (R=9.62) a(E)
0.3	0.865	0.419	0.577	0.516	0.298
0.4	0.929	0.348	0.723	0.685	0.450
0.5	0.956	0.283	0.808	0.770	0.552
0.8	0.982	0.206	0.911	0.893	0.744
1	0.987	0.172	0.937	0.923	0.806
1.5	0.993	0.119	0.964	0.956	0.884
2	0.995	0.101	0.975	0.970	0.920
3	0.997	0.075	0.985	0.982	0.949
4	0.9977	0.0518	0.9897	0.988	0.969
6	0.9986	0.0292	0.9939	0.993	0.982
8	0.999	0.0132	0.9959	0.9953	0.988
10	0.9992	0.0049	0.9969	0.9965	0.9911

According to these informations, when we multiply peak-to-total ratio with the total counts per seconds, we get the peak region counts per seconds for **theory 2**.

$$N \times ({}^{P}/_{T} = peak\ counts\ per\ seconds) \tag{3.15}$$

where,

N= total spectrum counts

P/T= peak to total ratio.

CHAPTER 4

EXPERIMENTS WITH CESIUM IODIDE SCINTILLATOR DETECTORS COUPLED WITH SILICON PHOTOMULTIPLIERS

4.1 Experimental Setup

A dark box is needed for the experiment because of that these experiments must be done in a dark ambient to get high sensitive of photons of the SPM detector. So that, the SPM and the scintillator were put into a black polyoxymethylene box. An optical glue was used as an optical interface between the scintillator and the SPMs. The read out electronics were connected to the box and the SPM inside. The schematic demonstration of the setup can be seen at **figure 4.1.**

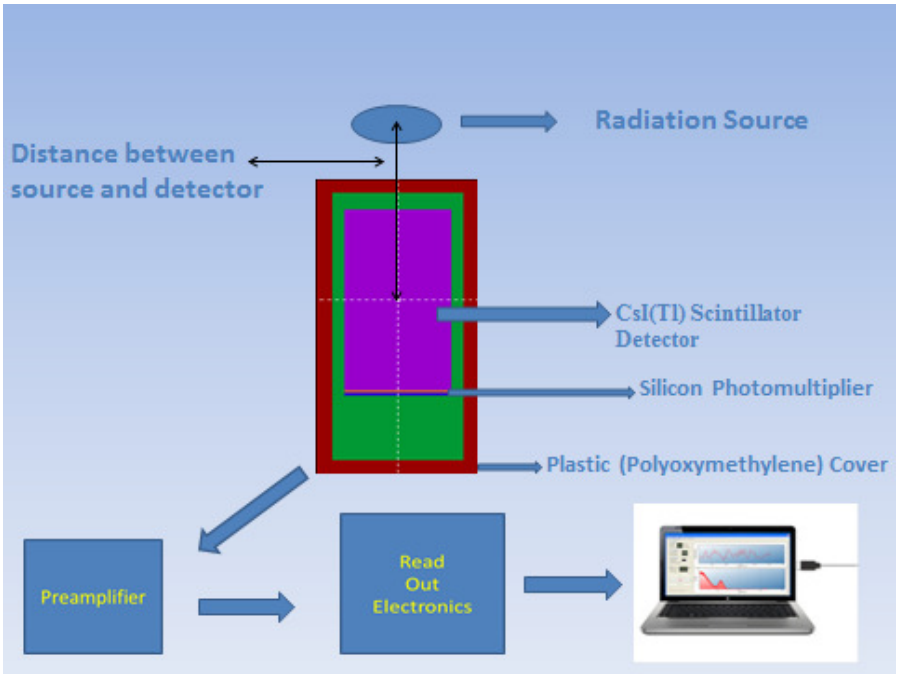

Figure 4.1: A schematic demonstration of the experimental setup.

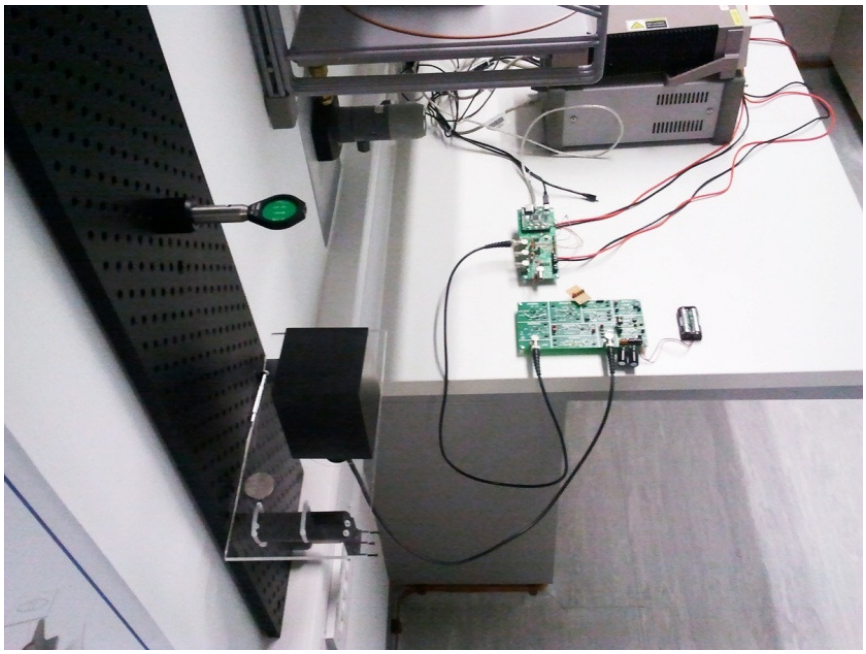

Figure 4.2: A picture of the experimental setup.

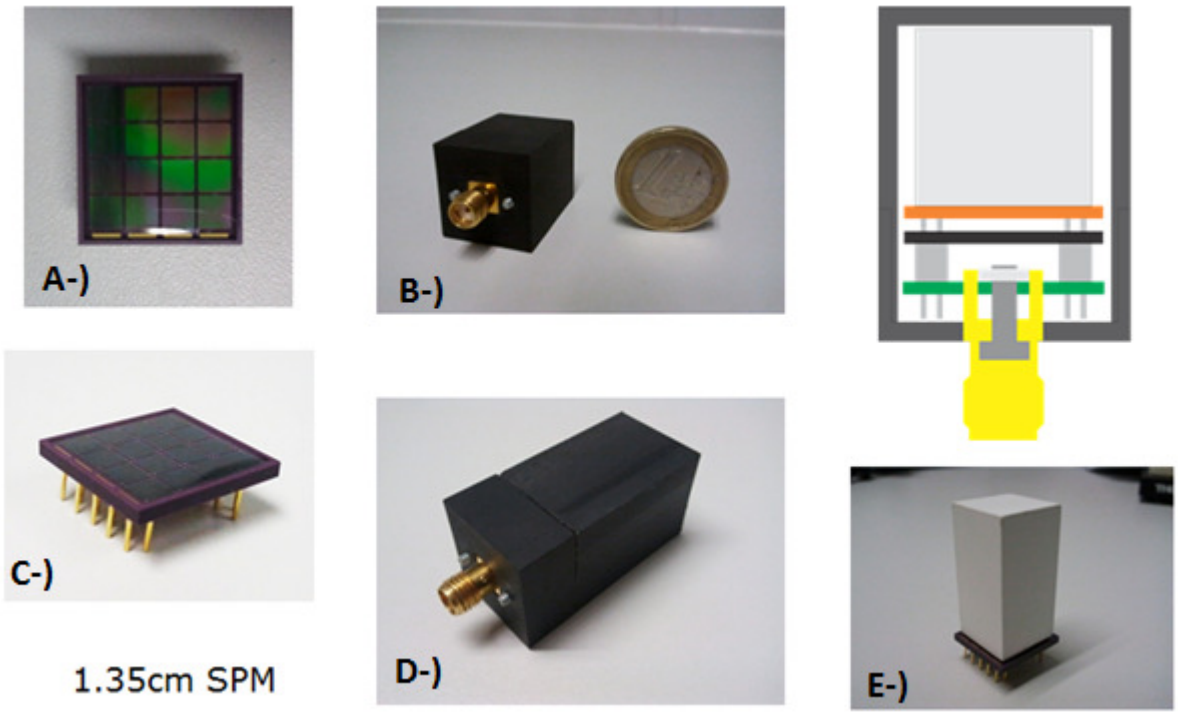

Figure 4.3: Pictures of the SPM(A-C), CsI(Tl) (E) and the polyoxymethylene cover (B-D).

4.2 Details of the radiation sources

We have used five type of point radiation sources, these are;

- **Am-241** (59.5 keV)
- **Ba-133** (80 keV and 356 keV)
- **Ge-68** (511 keV)
- **Cs-137** (662 keV)
- **Co-60** (1.17 MeV and 1.33 MeV)

4.3 Baseline Electronics

For the optimised detection of scintillation signals from CsI(Tl), it is required to use electronics which are optimised for the readout of SPM pixels and the signal response from CsI(Tl) crystal material. A set of modular electronics were developed for the optimised readout of SPM.

This modular readout approach allows for easy customisation and optimisation depending on the application. A block diagram of the signal chain used for the readout of scintillation crystals is shown in **figure 4.3**. This provides the baseline architecture for the electronics developed in this work.

Example of the signal chain for optimal readout of scintillation crystals with SPM. A preamplifier, shaper, variable gain amplifier to multi-channel analyser has proven to provide the most robust results for testing SPM sensor. This architecture was improved through the program to optimise for the intended application for low power and good sensitivity.

The read-out electronics developed to assess the probe functionality in terms of detecting radiation. These electronics consisted of a charge sensitive preamplifier, a digitally controlled RC shaper with variable gains and pulse shaping times and a commercial multi channel analyzer from in order to capture the signal height and hence the energy of the incoming radiation.

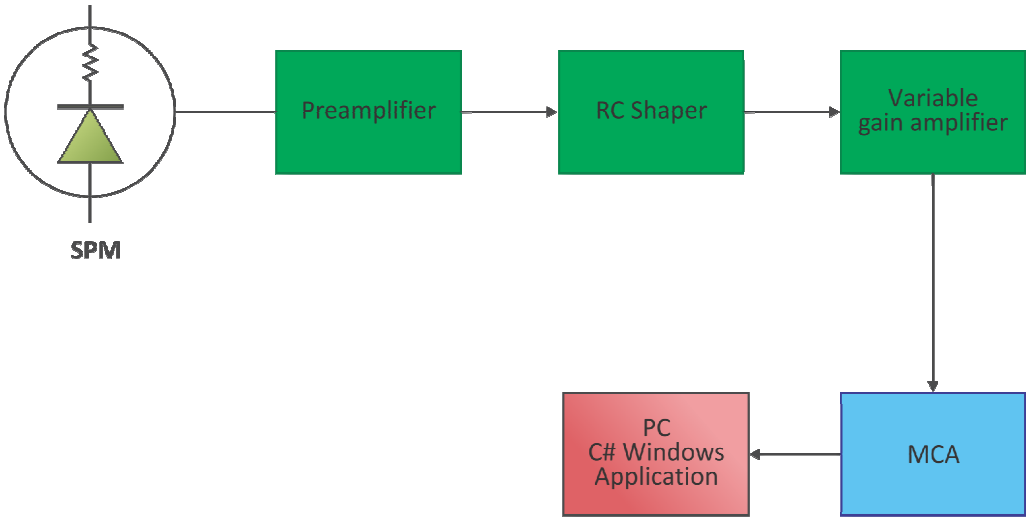

Figure 4.4: The schematic demonstration of the scintillator detector system used in experiments.

The signal pulse coming from the scintillation detector is so small that it will become impractical to deal with these signals without an intermediate amplification step. So we used the first element in signal processing chain is ”preamplifier” provided as the interface between detector and pulse processing and analysis electronics. The basic function of the preamplifier is to amplify the weaksignals coming from the detector and to direct it through the cable that connectsthe preamplifier with rest of the equipments. And the gain is controlled by a variable gain amplifier.

In order to increase the performance of a nuclear spectrometer and to reach high counting rate, shaping is required. In this process, differentiation and integration operation is made for eliminating the noise from the nuclear pulse. The optimization may be performed by several times integration although differentiation is made once.

The amplifier serves two main purposes:(i) Amplify the signal from preamplifier, and (ii) Shape it to convenient for further processing. In both cases, the amplifier must always preserve the information of interest. For spectroscopy amplifiers one of the most important factors is the pulse shaping characteristics. In general, the pulse coming from the preamplifier can be characterized as an exponential with a long tail lasting anywhere from τ to few μs - 100μs. The amplitude of the pulse is proportional to the energy.

Multichannel Analyzers are sophisticated devices which sort out incoming pulses according to pulse height and keep count of the number at each height in multichannel memory. The contents of each channel can then be displayed on a screen or printed out to give a pulse height spectrum. The MCA works by digitalizing the amplitude of the incoming pulse with ananalog to digital converter. The MCA takes this number and increments a memory channel whose address is proportional to the digitalized value. In this way incoming pulses are sorted out according to pulses height and the number at each pulse height stored in memory locations corresponding to these amplitudes.

CHAPTER 5

RESULTS AND DISCUSSION

The counts versus channel number values are obtained by using a standard multi-channel analyzer (MCA). However, it is necessary to make an energy calibration in order to determine the gamma energy in these channels. A good detection system gives a linear behavior which shows a well matching of channel number and gamma energy. But some deflections in linearity can be observed in detecting systems because of temperature dependence, the occurrence of radiation damage over time etc [27-29]. It is very important to calibrate the detection system in a wide energy spectrum in terms of determining the behavior of detector. Because these calibration curves are used for determine an unknown radiation source. For these reasons, some studies were performed in order to determine the energy calibration of CsI(Tl) and SPM combinations. Two different generations of SPM which are SL and SM were used for this reason. 30 Volt bias were applied to both detection systems. Each point source were put at 5 cm distance from the center of the CsI(Tl) crystal and energy spectrums obtained. The channel number corresponding to the maximum counts in the range of energy spectrum (photopeak peak point) were recorded and the energy calibration graphs were obtained

according to these values. **Figure 5.1** and **figure 5.2** demonstrates the energy calibrations of SM and SL generations respectively. The linearity levels (R^2=0.99878 and R^2=0.99845) of fitted lines are very close to 1. So that, the obtained calibration graphs are giving a well linearity behavior as expected from a good detector.

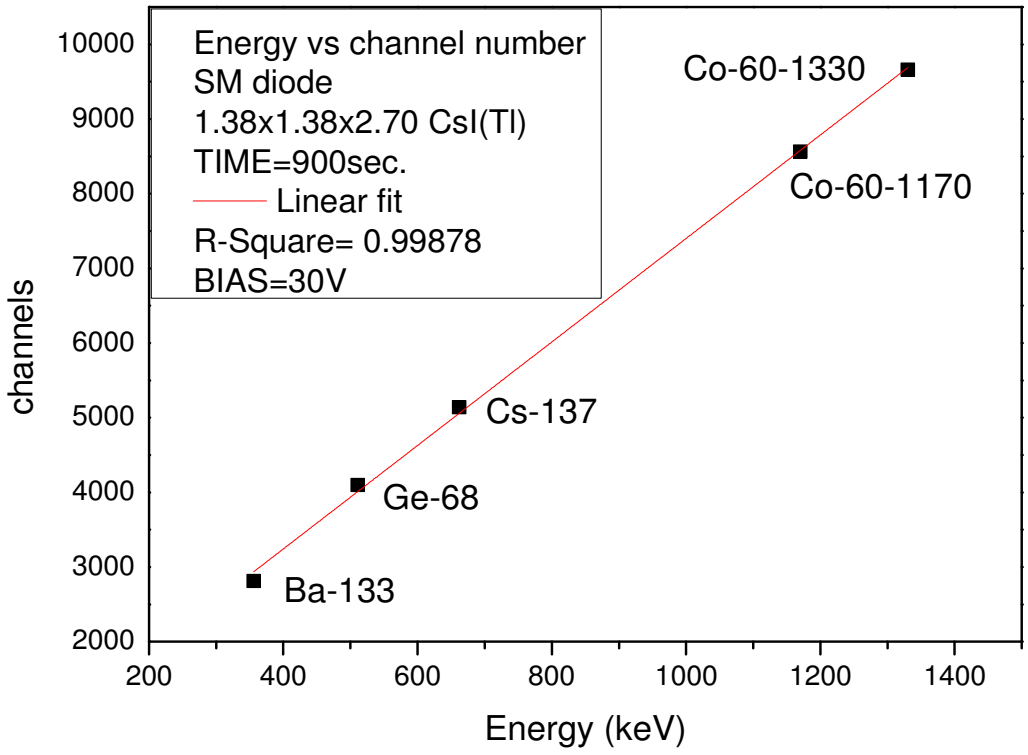

Figure 5.1: Energy calibration of 1.25 cm SM generation SPM.

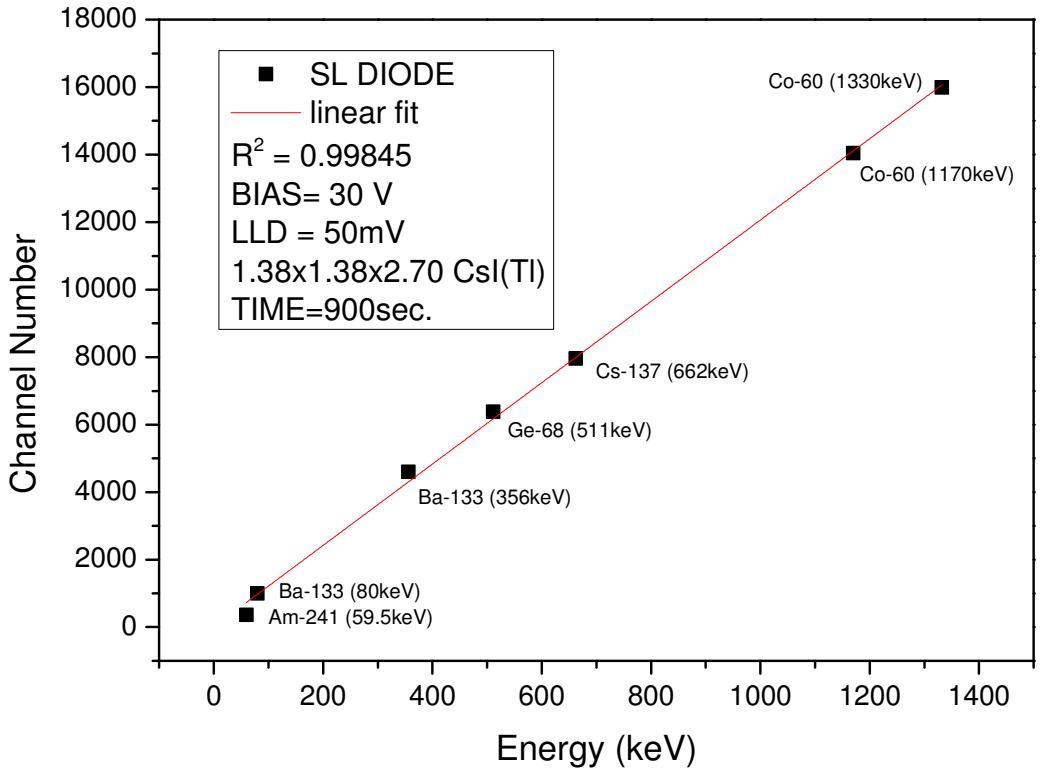

Figure 5.2: Energy calibration of 1.25 cm SL generation SPM.

Another important feature is expected in an ideal detector is good resolution. This means that the photopeak width obtained from an energy spectrum of a gamma source should be quite narrow. So that the photopeak generated by an unknown source can be seen in high definition. In addition to this feature, the noise ratio must be quite low. The energy spectrums of some different gamma sources obtained from a detector system including a CsI(Tl) crystal has dimensions 1.38x1.38x2.7cm and a SM generation SPM were demonstrated in **figure 5.3.** As seen on **figure 5.3**, 50mV LLD was applied to the system.

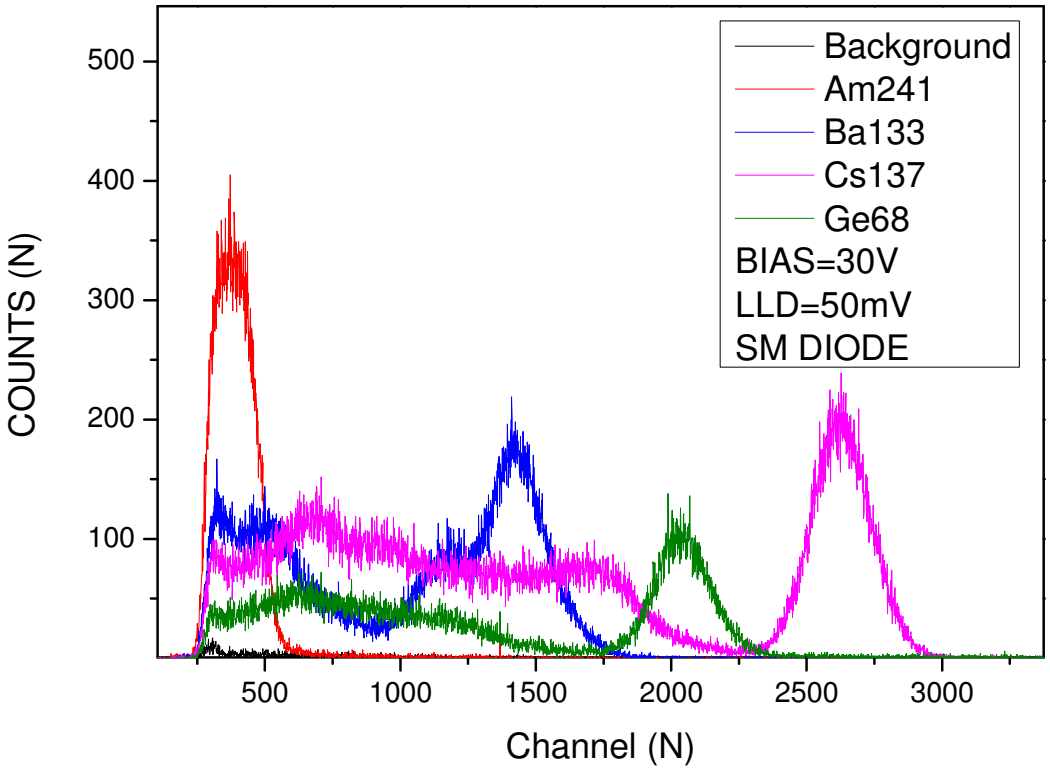

Figure 5.3: Total spectrum of some radioactive sources measured with 1.38cmx1.38cmx2.70cm CsI(Tl) scintillator using 50mV LLD.

As seen on the energy spectrums, the count values obtained from the Compton region are very high. Obtaining as small as count values from the Compton region is an expected property of an ideal detector. The most important reason of getting high counting values is the signal noise level is very high. This is a main important problem for interpretation of the activity of radionuclides having gamma peaks in low energy region such as Am-241. Energy resolution values show that the photopeak widths are very high. In order to reduce the noise level, some undesirable pulses can be eliminated.

The pulse below the set level are not analyzed by the lower level discriminator. (LLD) that provides to reject electronic noise and low energy X-Ray [30]. However, the detection efficiency of the system can be reduced with LLD. For this reason, a 32 Volt bias was used to protect the detection efficiency and a110 mVolt LLD was used to eliminate the undesirable electronic noise. The obtained energy spectrums were demonstrated in **figure 5.4.**

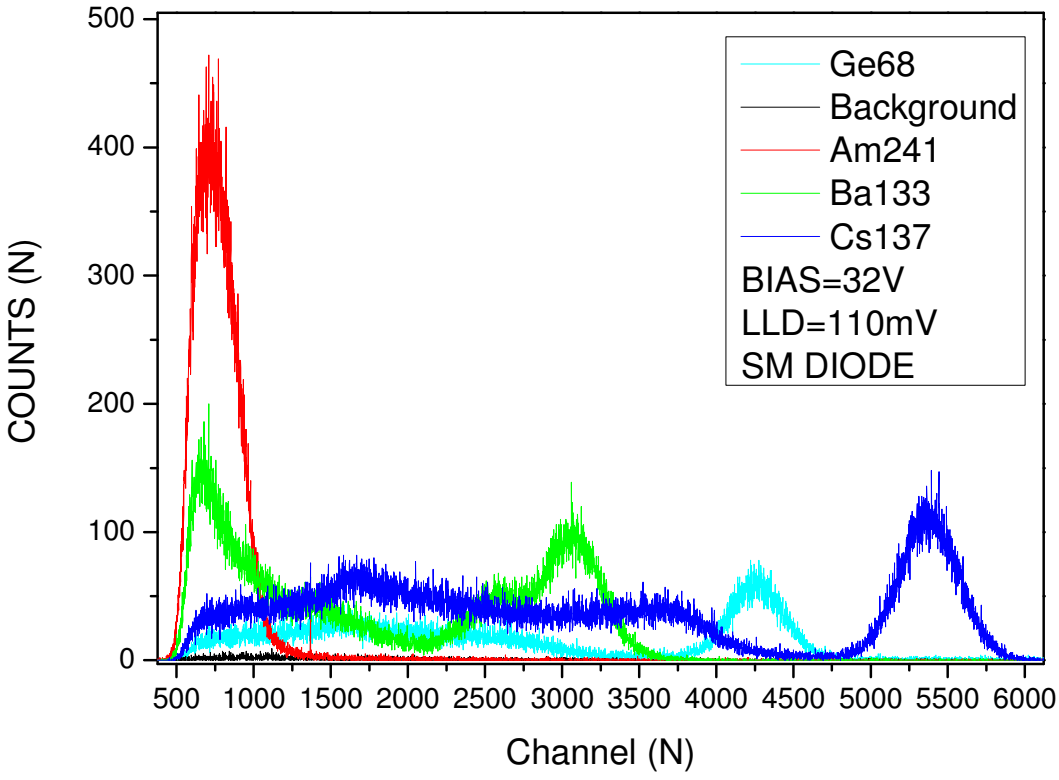

Figure 5.4: Total spectrum of some radioactive sources measured with 1.38cmx1.38cmx2.70cm CsI(Tl) scintillator using 110mV LLD.

The pulse heights of the photopeaks decreased by using 110 mV LLD. In addidition, the channel numbers of the photopeaks moved to the right side with increasing bias. In order to observe the voltage dependence of the photopeak channel number the experiments given in **figure 5.5** were performed. Obtained results show that the photopeak channel numbers increased with applied bias. As seen on the **figure 5.4,** the signal noise in the low energy level is increasing with the applied bias.

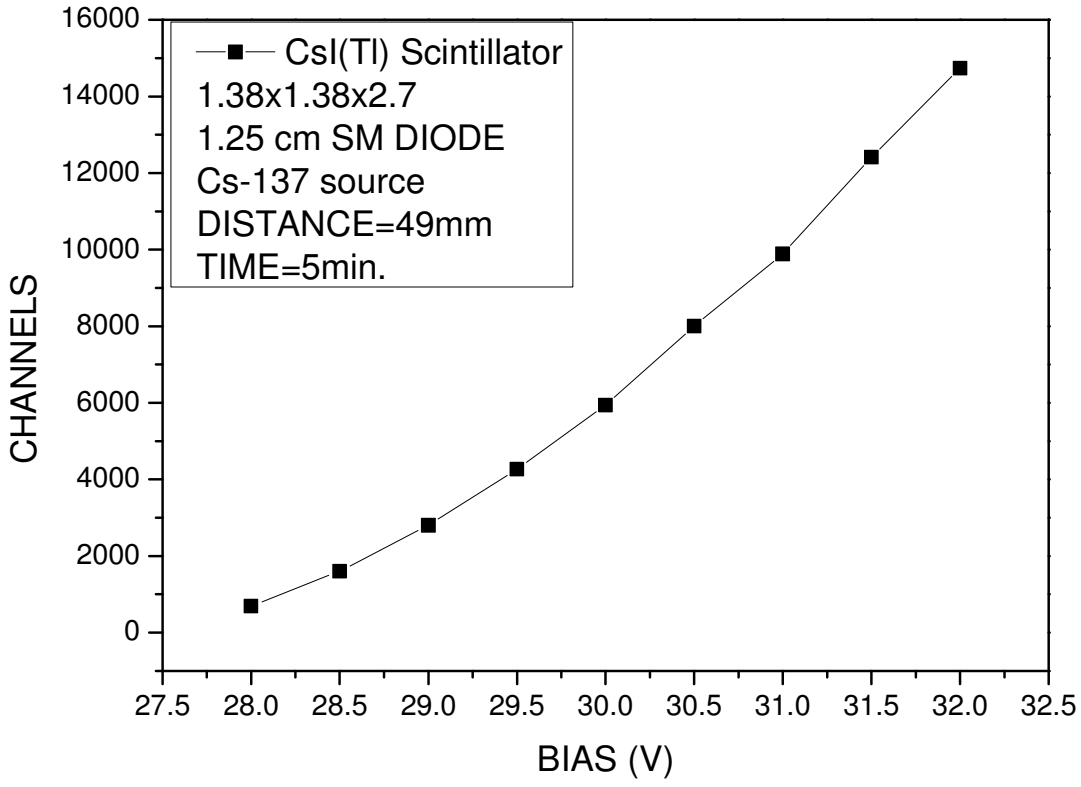

Figure 5.5: Applied bias vs. channel number.

As well as the applied voltage, temperature is another important parameter influencing the channel number corresponding to the photopeak[4]. In order to observe

this effect, the channel numbers corresponding to the photopic in different environment temperature using Cs-137 source were noted. Obtained changing graph is was demonstrated in figure 5.8. These results indicate that the photopeak channel shifted to the left side with increasing temperature.

Figure 5.6 shows the shift of the 662 keV photopeak for a temperature range between 19.9 °C and 23.1 °C for constant bias voltage (30V). Compared to results found in the literature, it can be easily said that the SPM is affected slightly by temperature variations. The read-out electronics and CsI(Tl) crystal are very sensitive to changing temperature, because of that a thermometer was put onto the electronic read-out circuit. Boatner et al. also reported the temperature dependence of the CsI(Tl) scintillator [31].

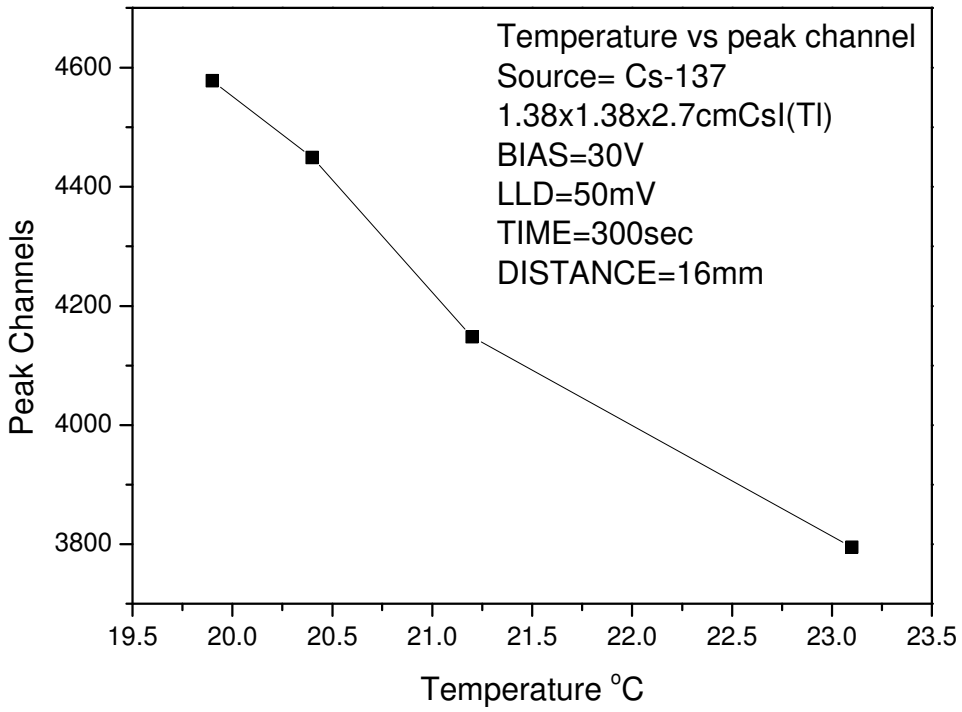

Figure 5.6: The temperature dependence of the photopeak of the Cs-137 source at 16mm.

Since measurements were taken without temperature stabilization, some deviations could be partially explained by time-to-time variations in room temperature. In contradistinction to its use for photon counting, the operating conditions of SPM are of primary concern when it is used as a light sensor in radiation detection due to the gain dependence on temperature and operating voltage. The optimization of these operational considerations directly affect the critical parameters and the performance of radiation detectors. [21]. The SPM and CsI(Tl) combinations operated good in room temperature. It is ovious that the noise and the gain are the parameters that is mainly affected. To develop correct dosimetry at changing temperatures this problem has to be solved. A fixing system working according to the relationship between temperature, bias and the gain may solve this problem. The temperature dependence of the photon detection efficiency was demonstrated in **figure 5.6** and **figure 5.7**. As seen on the **fig 5.7** the photopeak channel is moving to the left side with the increasing measured temperature.

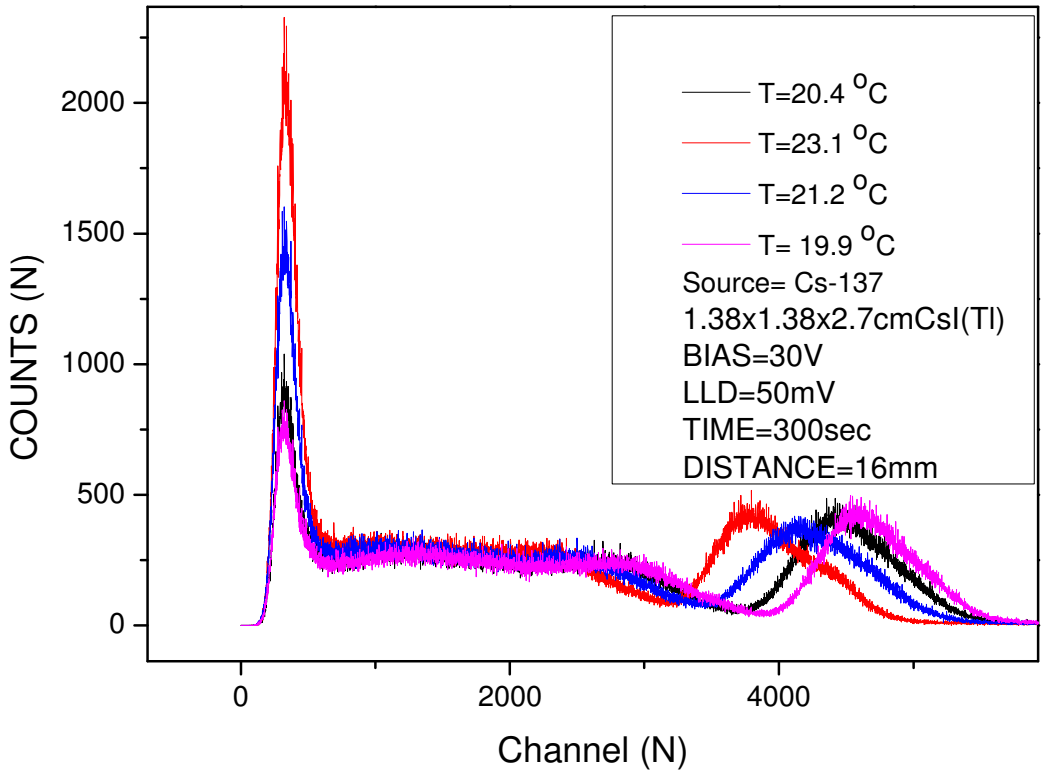

Figure 5.7: The temperature dependence of the photopeak of the Cs-137 source at 16mm.

In this part we gave the comparison of both of experimental total and peak counts per seconds and theoretical calculations. Am-241, Ba-133, Cs-137, Co-60 point radiation sources were used in these experiments. We used two different theories in comparing the results. The first theoretical calculations were obtained by using the efficiency calculations for scintillators guide [23]. And the second theoretical calculations were based on the Knoll and Cesena et al. [1,26].

Table 5.1 demonstrates the results of the measurements which were performed by using Cs-137 source and CsI(Tl) scintillator has a dimension of 1.38x1.38x2.7 cm. Peak fitting process were performed in two different channel gaps because of the temperature and noise dependence of the system. Even if a low temperature change effects the peak channels as seen on the **figure 5.6.** The total and photopeak counts were calculated for both gaps. The percentage errors for each calculation are small and close to each other. The reason of that we had big percentage errors for the total spectrum is the noise factor of the detection system and the background counts.

Table 5.2 and **Table 5.3** show the results of the measurements which were performed by using Co-60, Ba-133 sources and CsI(Tl) scintillator has a dimension of 1.38x1.38x2.7 cm. Co-60 has two gamma energies as 1.17 MeV and 1.33 MeV and Ba-133 has two gamma energies as 80 keV and 356 keV. It is difficult to separate the peaks while fitting because of that these peaks are very close. Consequently, the total counts of the measurements have big percentage errors comparing to the theories. But the peak counts agree with the theoretical values. 80 keV peak counts could not be separated because of the electronic noise. But it can be said that the total counts per second value has also the counts of 80keV gamms energy of the Ba-133.

The result of the experiment of Am-241 source can be seen in **Table 5.4.** The first 50 channels of the MCA were cut because of the electronic noise exists in this gap substantially. Am-241 measurements were assessed with just the first theory because of that the ***a(E)*** and ***b(E)*** values could not found in the literature [26]. But the percentage error is small.

Table 5.5 demonstrates the results of the measurements which were performed by using Ge-68 source and CsI(Tl) scintillator has a dimension 5.5x5.5x7.0 cm. Results

are in agood agreement with the theoretical values. The difference between the experimental and theoretical values is the result of the electronic noise and scattering from surrounding materials in laboratory.

Origin analyzing program was used in order to fit the line of the photopeaks.

- According to spectras and comparing tables, we have big differences in total counts more than peak counts. We get a big scattering region in spectras.
- We are getting more difference between experimental total counts per seconds and theoretical calculated counts per seconds because of the electronic noise and scattering from surrounding materials in laboratory.
- But in peak calculations, we get very close results with theory. This says to us we have a good counting system consists CsI(Tl) scintillator, silicon photomultiplier and read-out electronics.
- So, if the noise and temperature dependence of the system can be decreased, silicon photomultiplier arrays coupled with scintillators are an interesting candidate for detection of gamma radiation.

Table 5.1: Comparing theoretical and experimental counts per second values of Cs-137 source.

Cs-137	From Middle Point of the CsI(Tl) Scintillator, Date: 4.17.2013			
Distance (cm)	32.4		32.4	
Det. Dim. (cm)	1.38x1.38x2.7		1.38x1.38x2.7	
Time=1800sec	Peak Narrow	Total 1	Peak Wide	Total 2
Channels	(2740-4100)	(250-16383)	(2540-4300)	(300-16383)
Measurement (cps)	2.28	13.88	2.199	13.67
Theory 1 (cps)	2.54	8.46	2.54	8.46
Error 1 (%)	10.15	64.10	13.34	61.61
Theory 2 (cps)	2.66	8.27	2.66	8.27
Error 2 (%)	14.14	67.91	17.19	65.37

Table 5.2: Comparing theoretical and experimental counts per second values of Co-60 source.

Co-60	From Middle Point of the CsI(Tl) Scintillator, Date: 4.18.2013							
Distance (cm)	9.4				9.4			
Det. Dim. (cm)	1.38x1.38x2.7				1.38x1.38x2.7			
Energy	1173 keV				1332 keV			
Time=1800sec	Narrow Peak	Total	Wide Peak	Total	Narrow Peak	Total	Wide Peak	Total
Channels	2600-6720	250-16383	2400-6920	300-16383	2600-6720	250-16383	2400-6920	300-16383
Measurement (cps)	18.61	233.87	21.34	232.048	12.5	233.87	15.95	232.048
Theory 1 (cps)	18.07	100.41	18.07	100.41	15.98	94.00	15.98	94.00
Error 1 (%)	2.96	132.91	18.07	131.10	21.78	148.79	0.19	146.85
Theory 2 (cps)	18.29	102.10	18.29	102.10	15.30	96.79	15.30	96.79
Error 2 (%)	1.73	129.05	16.65	127.27	18.29	141.64	4.26	139.75

Table 5.3: Comparing theoretical and experimental counts per second values of Ba-133 source.

Ba-133	From Middle Point of the CsI(Tl) Scintillator, Date: 4.23.2013			
Distance (cm)	16.7		16.7	
Det. Dim. (cm)	1.38x1.38x2.7		1.38x1.38x2.7	
Time=1800sec	Peak Narrow	Total 1	Peak Wide	Total 2
Channels	(1085-2750)	(250-16383)	(885-2950)	(300-16383)
Measurement (cps)	7.78	29.92	8.05	28.01
Theory 1 (cps)	6.90	13.79	6.90	13.79
Error 1 (%)	12.81	116.91	16.72	103.07
Theory 2 (cps)	7.87	14.14	7.87	14.14
Error 2 (%)	1.13	111.61	2.30	98.10

Table 5.4: Comparing theoretical and experimental counts per second values of Am-241 source.

Am-241	From Middle Point of the CsI(Tl) Scintillator, Date: 4.18.2013	
Distance (cm)	5.4	
Det. Dim. (cm)	1.38x1.38x2.7	
Energy	59.5 keV	
Time=1800sec	Peak	Total
Channels	0-800	50-16383
Theory 1 (cps)	686.59	686.59
Error 1 (%)	4.51	12.41

Table 5.5: Comparing theoretical and experimental counts per second values of Ge-68 source.

Ge-68	From Middle Point of the CsI(Tl) Scintillator, Date: 28.3.2013	
Distance (cm)	30	
Det. Dim. (cm)	5.5x5.5x7.0 cm CsI(Tl) scintillator	
Time=3600sec	Peak	Total
Channels	(410-73	0-16383)
Measurement (cps)	62.98	97.27
Theory 1 (cps)	59.48	90.13
Error 1 (%)	5.37	7.93
Theory 2 (cps)	59.61	91.41
Error 2 (%)	5.15	6.41

Table 5.6: Comparing table of errors of peak and total counts.

Source	Distance (cm)	Peak Counts Error		Total Counts Error (%)	
		Theory 1	Theory 2	Theory 1	Theory 2
Cs-137	32.4	10.15	14.14	64.10	67.91
Cs-137	14.1	3.16	11.43	97.75	98.06
Ge-68	30	5.37	5.15	7.93	6.41
Am-241	5.4	4.51		12.41	
Ba-133	16.7	12.81	1.13	116.91	111.61
Co-60 1173 keV	9.4	2.96	1.73	132.91	129.05
Co-60 1332 keV	9.4	0.19	4.26	146.85	139.75

We compared some experimental counting results with two theories. Unlike peak counts, comparing tables show that we get more differences in total counts than peak counts. **(See table 5.6).** We are getting more difference between experimental total counts per seconds and theoretical calculated counts per seconds because of the electronic noise and scattering from surrounding materials in laboratory. Obtained peak counts calculations are very close to theoretical values generally. This says to us we have a good counting system consists CsI(Tl) scintillator, silicon photomultiplier and electronic system.

Radiation detection with scintillators is a traditional technique. PMT technology have been used for scintillation process for many years. To date the PMT, a well established and widely available vacuum tube device, has been the detector of choice for such applications. A gain of 1-10e^6 is achieved at the cost of a high bias voltage of 1-2kV, which requires the use of costly high-voltage power supplies with PMTs high cost, vacuum technology and sensitivity to magnetic fields which limit their suitability for some applications [5,17,32]. PMTs are generally stable and low noise but are bulky and delicate due to their vacuum tube structure.

The SPM device has good gain and moderate photon detection efficiency approximately 20%. It is very similar to the PMT technology, but PMT has the physical disadvantages of compactness, ruggedness and magnetic sensitivity. In addition, the SPM achieves its high gain (10^6) with very low bias voltages approximately 30V and the noise is almost entirely at the single photon level as in our experiments performed. The ability to measure a good resolved photoelectron spectrum is a feature of the SPM which is generally not possible with PMTs due to the variability in the gain, or excess noise[20].

CHAPTER 6

CONCLUSIONS

Characteristics of CsI(Tl)-SPM detector has been investigated for the gamma rays emitted by the Am-241, Ba-133, Cs-137 and Co-60 radioactive sources. CsI(Tl) has a larger gamma-ray absorption coefficient compared to other inorganic scintillators. It is found that the CsI(Tl)-SPM combination has a good performance.

There are many advantages of SPMs to replacing PMT technology. Compared to the glass enclosed PMT, the SPM is much smaller and orders of magnitude more rugged. SPM also offers a much greater dynamic range, with a linear response over 10^6. Applied operating voltages are much lower, typically about 30 V, as opposed to several hundred, or up to 1000 V, in a PMT. One of the biggest advantage of the SPM device is its high quantum efficiency. In a typical PMT only 10-25% of incident photons generate photoelectrons at the photocathode. But the SPMs can have quantum efficiencies as high as 90% in the visible light spectrum. SPMs are also virtually insensitive to magnetic fields. Although PMTs are the most widely used devices until now, new technological advances have made possible the development of semiconductor SPMs for use with scintillator detectors as well. In conclusion, according to the present results and the

literatural knowleges, it is obvious that the SPM technololgy must replace the PMT technology.

REFERENCES

[1] G.F. Knoll, Radiation Detection and Measurement, John Wiley & Sons, Inc., 2000.

[2] M. Moszynski, Nucl Instrum Meth A 505 (2003) 101.

[3] M. Jönsson, Masters, CHALMERS UNIVERSITY OF TECHNOLOGY, Göteborg, Sweden, 2010.

[4] C. Degenhardt, G. Prescher, T. Frach, A. Thon, R. Gruyter, A. Schmitz, R. Ballizany, The Digital Silicon Photomultiplier – A Novel Sensor for the Detection of Scintillation Light, 2009 IEEE Nuclear Science Symposium Conference, 2009.

[5] D. Renker, Nucl Instrum Meth A 567 (2006) 48.

[6] E.M. Becker, A.T. Farsoni, A.M. Alhawsawi, B. Alemayehu, Ieee T Nucl Sci 60 (2013) 968.

[7] D.R. Schaart, S. Seifert, R. Vinke, H.T. van Dam, P. Dendooven, H. Lohner, F.J. Beekman, Phys Med Biol 55 (2010) N179.

[8] N. Serra, A. Ferri, A. Gola, T. Pro, A. Tarolli, N. Zorzi, C. Piemonte, J Instrum 8 (2013).

[9] E. Yilmaz, DOCTOR OF PHILOSOPHY, MIDDLE EAST TECHNICAL UNIVERSITY, 2003.

[10] C.L. Templeman, The Compton Effect. The College of Wooster, Wooster, Ohio, 2000, p. 4.

[11] R.M. Preston, J.E. Eberhardt, J.R. Tickner, Ieee T Nucl Sci 61 (2014) 2410.

[12] H.P. K.K., Photomultiplier Tubes Basics and Applications, Hamamatsu Photonics K.K., 2006.

[13] T. Szczesniak, M. Grodzicka, M. Moszynski, M. Szawlowski, D. Wolski, J. Baszak, Nucl Instrum Meth A 702 (2013) 91.

[14] M. Janecek, J.P. Walder, P.J. McVittie, B. Zheng, H. von der Lippe, M. McClish, P. Dokhale, C.J. Stapels, J.F. Christian, K.S. Shah, W.W. Moses, Ieee T Nucl Sci 59 (2012) 13.

[15] C. Tur, V. Solovyev, J. Flamanc, Nucl Instrum Meth A 620 (2010) 351.

[16] P. Buzhan, B. Dolgoshein, L. Filatov, A. Ilyin, V. Kantzerov, V. Kaplin, A. Karakash, F. Kayumov, S. Klemin, E. Popova, S. Smirnov, Nucl Instrum Meth A 504 (2003) 48.

[17] V.D. Kovaltchouk, G.J. Lolos, Z. Papandreou, K. Wolbaum, Nucl Instrum Meth A 538 (2005) 408.

[18] S. Seifert, H.T. van Dam, R. Vinke, P. Dendooven, H. Lohner, F.J. Beekman, D.R. Schaart, Ieee T Nucl Sci 59 (2012) 190.

[19] D.J. Herbert, S. Moehrs, N. D'Ascenzo, N. Belcari, A. Del Guerra, F. Morsani, V. Saveliev, Nucl Instrum Meth A 573 (2007) 84.

[20] SensL, Introduction to the SPM. SensL Light, 2011, p. 8.

[21] D. Ginzburg, N. Kopeika, J. Paran, I. Cohen-Zada, M. Ghelman, V. Pushkarsky, E. Marcus, A. Manor, T. Mazor, Y. Kadmon, Y. Cohen, A. Osoyizky, Nucl Instrum Meth A 652 (2011) 474.

[22] H. Sabet, H.B. Bhandari, H. Kudrolli, S.R. Miller, V.V. Nagarkar, Ieee T Nucl Sci 60 (2013) 1000.

[23] Efficiency Calculations for Selected Scintillators. BICRON-crismatec, 2004.

[24] W. contributors, Scintillator Counter. Wikipedia, The Free Encyclopedia.

[25] T.N.I.o.S.a.T. (NIST), Mass Attenuation Coeffcient table of Cesium Iodide. The National Institute of Standards and Technology (NIST), 2014.

[26] A. Cesena, M. Terrani, Nuclear Instruments & Methods in Physics Research A 281 (1989) 172.

[27] E. Garutti, R. Klanner, S. Laurien, P. Parygin, E. Popova, M. Ramilli, C. Xu, J Instrum 9 (2014).

[28] M. Niu, C.M. Kao, J. Zhu, P. Xiao, A. Long, R.G. Wagner, G. Drake, C.T. Chen, Q. Xie, J Instrum 7 (2012).

[29] G.C. Wang, J.S. Huber, W.W. Moses, W.S. Choong, J.S. Maltz, Ieee T Nucl Sci 51 (2004) 775.

[30] G. Gilmore, Practical Gamma-ray Spectrometry, John Wiley & Sons, Ltd. , UK, 2008.

[31] L.A. Boatner, J.S. Neal, J.A. Kolopus, J.O. Ramey, H. Akkurt, Nucl Instrum Meth A 709 (2013) 95.

[32] J. Gal, G. Kalinka, B.M. Nyako, Nucl Instrum Meth A 607 (2009) 607.